Tracking Trash to Treasure: In situ monitoring of Single Microbial Cell Oil biosynthesis from Waste Cooking Oil using Raman Reverse Isotope Probing and Imaging

Jiro Karlo[a], Victor Carrasco-Navarro[b], Arto Koistinen[c], Surya Pratap Singh[a]*
[a]Department of Biosciences and Bioengineering, Indian Institute of Technology Dharwad, Dharwad, Karnataka, India - 580011
[b]Department of Environmental and Biological Sciences, University of Eastern Finland, Kuopio Campus, Yliopistonranta 8, Kuopio, Finland – 70210
[c] Department of Technical Physics, University of Eastern Finland, Kuopio, Finland - 70210
*Corresponding Author, *e-mail:* ssingh@iitdh.ac.in

Abstract:

Single microbial cell oil (SMCO) plays a fundamental role in maintaining the structure of cellular membranes and as energy reservoirs. Oleaginous microbes are known to have a high content of lipids, which often acts as a microbial factory for the bioremediation of waste cooking oil (WCO) which is a major pollutant contaminating land and water bodies. The biomass of microbes grown in WCO can be utilized to develop sustainable value-added products such as biodiesel, organic chemicals, bio preservatives, biosurfactants biopolymers. Conventional methods excel in SMCO analysis but lack efficacy for in situ or lysis-free monitoring of nascent SMCO synthesis and its turnover dynamics. To bridge this knowledge gap, in this study we have employed Raman reverse stable isotope probing (RrSIP) to investigate the time dependent nascent SMCO synthesis and assimilation in *Yarrowia lipolytica,* a well-known oleaginous yeast. Our finding provides a unique perspective for utilizing optical spectroscopy methods for lysis-free SMCO analysis which holds potential for utilization as an adjunct tool in bioprocess and biofuels industries.

Graphical Abstract:

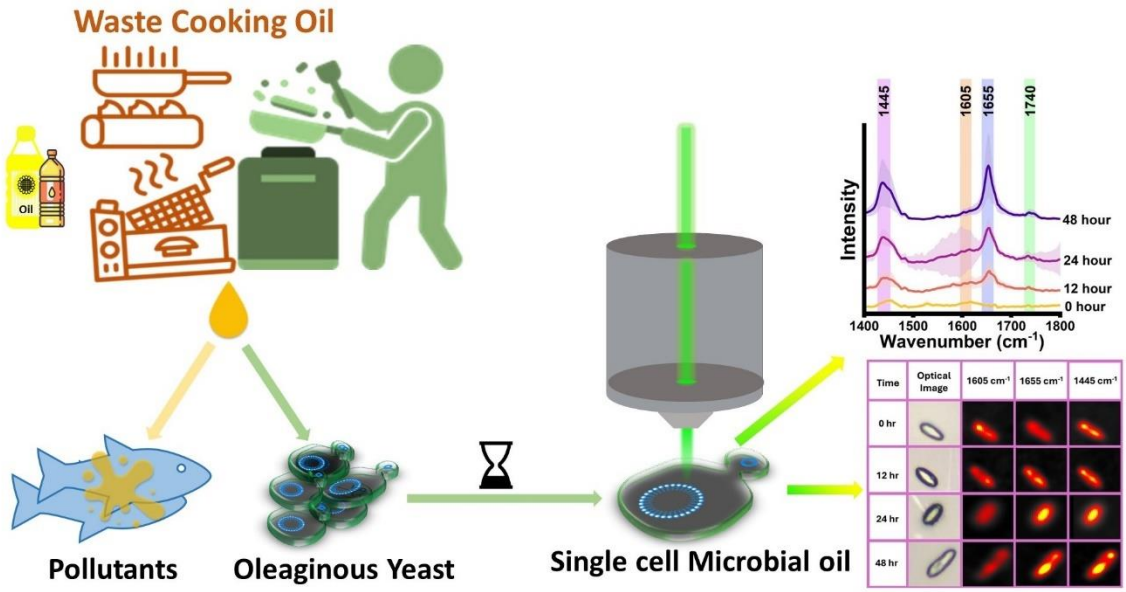

1. Introduction:

Waste cooking oil (WCO) generated all over the world in domestic kitchens, food processing industries, restaurants, and others is considered as one of the major environmental pollutants.[1] Unprocessed WCO is a major concern when it is disposed in water bodies and land which forming oily sludge and contaminating terrestrial and aquatic habitats. In addition, reusing it for cooking has a hazardous impact on health. [2,3] As per previously reported studies each year global WCO production is estimated to be around 15 million tons.[4,5] WCO due to its relatively simple chemical composition, primarily consisting of triglyceride esters of glycerol with long fatty acid chains mainly oleic acid (C18:1) and linoleic acid (C18:2) makes it a valuable feedstock from the industrial perspective.[6] Multiple studies have reported its utility to produce value-added products such as biodiesel, bioplastics, biogas, biosurfactants, biopolymers, lubricants, and others which promotes "circularity and sustainability".[4,6–10] The bioremediation of WCO has been done via oleaginous microorganisms and the biomass of oleaginous yeast has become one of the increasingly favoured for sustainable value-added products in industries as it has a fast growth rate, the inherent ability of lipid storage, requires less labour and is highly scalable.[11] In our study we have used *Yarrowia lipolytica (YL)*, an oleaginous yeast which can synthesize important metabolites such as microbial oil containing high levels of unsaturated fatty acid, lipases, proteases and others.[12] Bioprocess based on YL is categorised as GRAS (Generally Recognised As Safe) by the Food and Drug Administration (FDA, USA).[13,14] Due to its capability of synthesizing extracellular lipases it stands out among yeasts to metabolize hydrophobic substrates such as WCO. Few of the reported YL strains have the potential to accumulate lipids more than 30-45% of their dry weight.[11] The accumulation of the lipids in oleaginous microbes is mostly in the form of triacyl glycerides (TAGs) with YL strains reported to contain 88-89% of its total lipid content .[15,16] TAGs are the neutral lipids which are the most suitable form of lipid for direct conversion to biodiesel.[16] In yeast, neutral lipids are stored in lipid bodies (LBs) also known as lipid droplets but it also maintains a significant portion of free fatty acids and sterol esters .[17,18]

In the previously reported studies, SMCO analysis has been performed using highly efficient methods such as Gas Chromatography-Mass Spectrometry (GC-MS) and Gas Chromatography Flame Ionization Detection (GC-FID). Determination of fatty acid profile and quantification with high sensitivity and reproducibility has been achieved.[16,19–21] However, these methods require extraction of the lipids from cells which cannot be applied for *in-situ* temporal monitoring of the nascent SMCO turnover dynamics of microbial oil synthesis and accumulation at single cell level. Fluorescence spectroscopy is another technique for SMCO analysis using external fluro-probes.[22–25] Intracellular SMCO estimation and localization are done using fluorescence microscopy and spectrofluorimetry.[16,26] Lipid bodies of YL have been analysed in many previous studied using fluorescence imaging. [16,23,25,27] Nile red and BODIPY are the most used probes for lipids. However, these probes cannot provide distinctions between specific SMCO saturation and unsaturation components. Another semi-quantification method of determining lipids in YL is Flow cytometry using fluorescence intensity for detecting the amount of intracellular lipid bodies.[26]. Microbial metabolites can also be analysed by stable isotope probing using the two known techniques, Secondary Ions Mass Spectrometry (SIMS) and Raman spectroscopy.[28] SIMS is a highly sensitive but destructive method.[28,29].

To maximize the utilization of oleaginous microbes for bioremediation of WCO as efficient biomass in the bioprocess and biofuel industries, understanding the carbon flow, synthesis, and accumulation of SMCO at the single cell level in lysis-free approach is much needed. Through this study we propose the prospective utility of Raman spectroscopy methods in combination with reverse stable isotope probe (RrSIP) for the lysis-free temporal monitoring of SMCO synthesis and its turnover dynamics at the single-cell level.[30–32]. In this approach, the ^{13}C stable isotope-labelled cells are inoculated and grown in presence of ^{12}C unlabelled source containing culture medium. With the metabolic incorporation of unlabelled carbon in the newly synthesized metabolites, there is a decrease in reduced mass which leads to an increase in the wavenumber also known as blue shift of the spectral bands. Monitoring of this shifted unlabelled band position can serve as the spectral indicator for dynamic monitoring of nascent metabolites and unlabelled peak positions are well reported in literature. Further, WCO is inherently a source of unlabelled carbon contributing to the effectiveness of the RrSIP methodology. As the unlabelled carbon sources have higher natural abundance this approach becomes cost-effective. [30–33] In previous studies, the SMCO composition of YL has been reported to be predominated by long-chain unsaturated fatty acids (UFA) which makes it a potential candidate for industrial use.[14,34,35] As UFA is an integral part of SMCO composition, we have used the unsaturated fatty acid Raman band as our representative spectral tracer for in situ SMCO analysis. We have monitored *de novo* and *ex novo* synthesis of SMCO using hydrophilic and hydrophobic sources as shown in **Fig. 1**. After validating the nascent UFA band as a lysis-free tracer for SMCO analysis, we have evaluated its applicability for monitoring converting WCO.

2. Material and Methods:

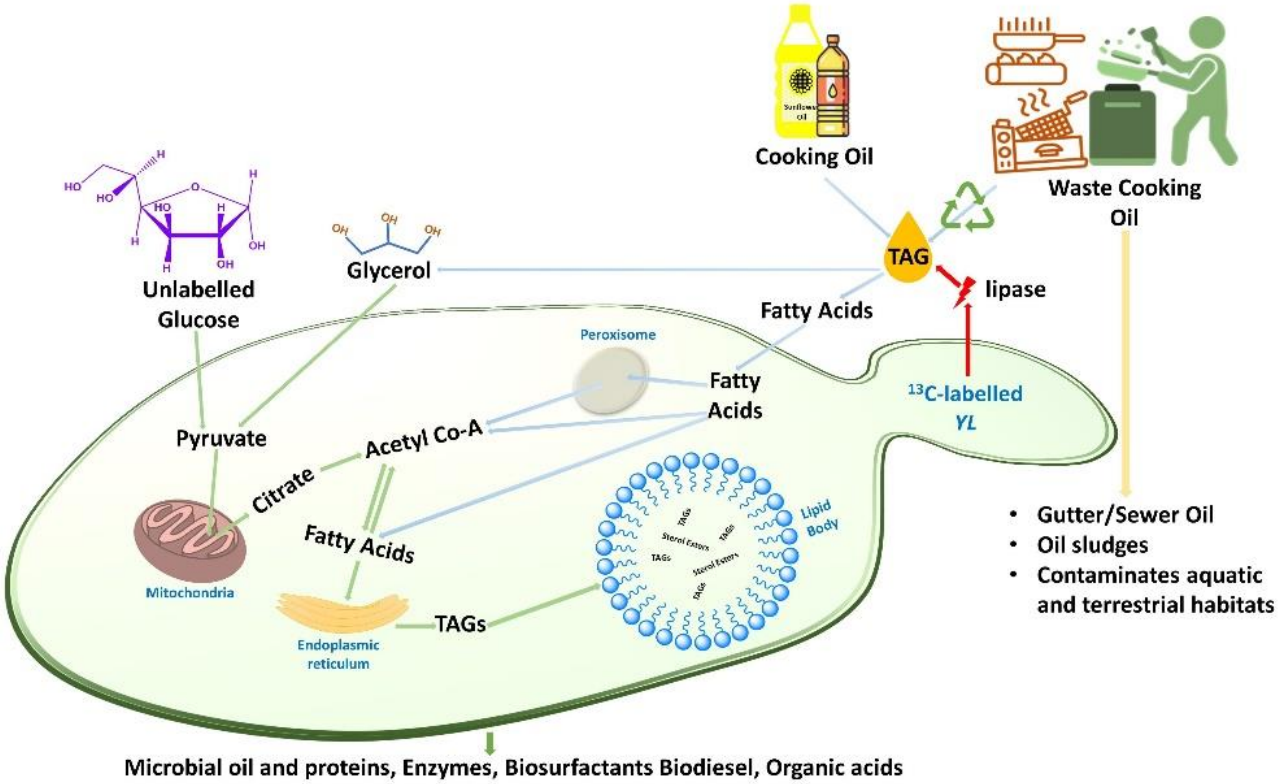

Fig 1. Schematic representation of denovo and exnovo synthesis of single microbial cell oil pathways in Yarrowia lipolytica from different hydrophillic and hydrophobic carbon source.

2.1. Yeast Culture

Oleaginous yeast strain *Yarrowia lipolytica* NCIM 3472 was purchased from the National Collection of Industrial Microorganisms, Pune, India. YL was pre-cultured in a carbon-deficient synthetic broth medium (Sigma Aldrich) and supplied with 10 g/L glucose (Sigma Aldrich). Incubation parameters for the growth were set with the temperature at 28° ℃ and the rotational shaker set at 180 RPM. The growth evaluation of YL in a synthetic medium supplemented with unlabelled and uniformly labelled ^{13}C glucose (99%, Cambridge Isotope Laboratories) was performed using Optical density at 600 nm (OD_{600}) using UV-1900i UV-Vis Spectrophotometer (Shimadzu) at multiple incubation time interval (2x). For performing an inhibition assay, Cerulenin (Sigma Aldrich) a well-known fatty acid synthase inhibitor (50 µg/ml) was used. To reverse the effect of the inhibition assay, exogenous mono and polyunsaturated fatty acid supplements (oleic and linoleic acid) were provided in 1:1 ratio. All the standard fatty acids were obtained from Sisco Research Laboratories. Yeast lipid extraction and protein extraction protocols were adapted from previous reports.[36,37] The Cooking oil namely palmolein and sunflower oil was purchased from a local vendor and waste cooking oil was provided by a local eatery from IIT Dharwad. Oil samples (100 g/L) were sterile syringe filtered before supplementing to the synthetic media as the sole carbon source before inoculation.

2.2. Sample preparation, Single-cell Raman spectroscopy and data analysis:

For the Single-cell RrSIP experiments, the aliquots were washed with 1x-phosphate buffer saline (PBS, Sisco Research Laboratories). To obtain individual single cells on the ethanol washed slide appropriate dilutions were performed at different time intervals. WITec confocal micro-Raman spectrometer, equipped with a 532 nm laser source and 100× objective lens was used to acquire a single spectrum from each cell. Each spectrum acquired was averaged over 5 accumulations with a 20-second exposure time. The MATLAB software version R2021B was used for processing the spectral data. Denoising of the spectral data was done using the Savitzky Golay filter, baseline corrected with 5th order polynomial and unit normalized. The mean spectra along with standard deviation and all the other plots were generated using Origin Pro 2023b Software.

2.3. Single-cell Raman imaging and analysis:

The single cell was obtained and mounted on a Calcium fluoride substrate as per the previously mentioned procedure[28]. For the Raman imaging using WITec confocal micro-Raman spectrometer, the step size of the scan was kept at around 0.3 microns with a 5 second laser exposure time. The Raman hyperspectral imaging spectral data was pre-processed via routine procedures involving denoising, baseline correction and normalization. Raman images based on SMCO tracer bands were generated using in-house codes and k means cluster analysis using MATLAB 2021B software.[38] Other plots related to hyperspectral data were generated using Origin Pro 2023b Software.

3. Results and Discussions:

3.1. In situ Monitoring *de novo* synthesis of single microbial cell oil and its turnover using unsaturated fatty acid band as the tracer

Unsaturated fatty acid is an integral part of single microbial cell oil composition. In a previously reported study, the SMCO content of YL 3472 when compared to other YL strains was reported to have the highest content of monounsaturated fatty acid grown in glucose

and the highest polyunsaturated fatty acid content grown in waste cooking oil.[16] Band position at 1655 cm^{-1} and 1605 cm^{-1} (cis C=C stretching vibration) in the Raman spectra of cells have been reported as unlabelled and ^{13}C labelled unsaturated fatty acids. 1445 cm^{-1} has been used to analyse the total lipid pool which should be the ideal candidate for SMCO synthesis analysis, but this peak has not been reported to show any isotopic substitution shift to the best of our knowledge.[28,30,39–43]

Our first goal was to investigate the feasibility of the RrSIP methodology for SMCO analysis. We monitored the carbon flow from the carbon source, *de novo* UFA biosynthesis and turnover of the nascent UFA in a lysis-free approach at different time intervals. Firstly, we evaluated the growth pattern of YL grown in carbon source-free synthetic media supplemented with unlabelled and ^{13}C glucose using optical density measurements at different time points 0, 2, 5, 7, 9, 12, 24, 48 hours as shown in **Fig. S1(A)**. The growth pattern of the cells was seen to be similar to the cells growing in carbon-source rich media, confirming unaltered metabolic activity due to ^{13}C substitution. Average Raman spectra of single yeast cells along with standard deviation at different incubation time intervals (0, 2, 5, 7, 9, 12 and 24 hours) are shown in **Fig. 2(A)**. At 0 hours, the inoculated cells are ^{13}C-labelled, and we observed an intensified ^{13}C-labelled UFA band signal at 1605 cm^{-1} and a minor signal at 1655 cm^{-1} indicating that almost the entire SMCO UFA pool is ^{13}C-labelled. At 2 hours, we observe an increase in band intensity at the 1655 cm^{-1} region indicating the ^{13}C carbon flow from culture media to cell cytoplasm and active *de novo* UFA biosynthesis. At 5 hours we observed an equal intensity of 1605 cm^{-1} and 1655 cm^{-1}. With further increase in the incubation time, we observe an increase in the intensity at 1655 cm^{-1} while that of 1605 cm^{-1} goes down. At 24 hours, we observe a highly intense signal at 1655 cm^{-1} whereas at 1605 cm^{-1} becomes small, but the residual intensity remains as the position is slightly influenced by ergosterol at 1602 cm^{-1} and nearby biomolecular signals.[44] This shows that 1655 cm^{-1} band can be a possible tracer of nascent UFA, but further validation is required. Additionally, the ratiometric integrated intensity at 1655/1605 band position at different incubation time intervals provides a quantitative insight into metabolic carbon incorporation and turnover dynamics of nascent UFA. As shown in **Fig. 2(B)**, an increase in 1655/1605 is seen in earlier time points indicating the newly synthesized unlabelled UFA gradually replacing the old pool of UFA. The curve reaches a plateau in the late incubation hours indicating almost the entire old pool of UFA is substituted by the nascent UFA. **Fig. 2(C)** shows ratiometric intensity changes in 1655/1445 showing the turnover of nascent UFA in the total lipid pool of the single YL cells. However, this time-dependent blueshift of the UFA

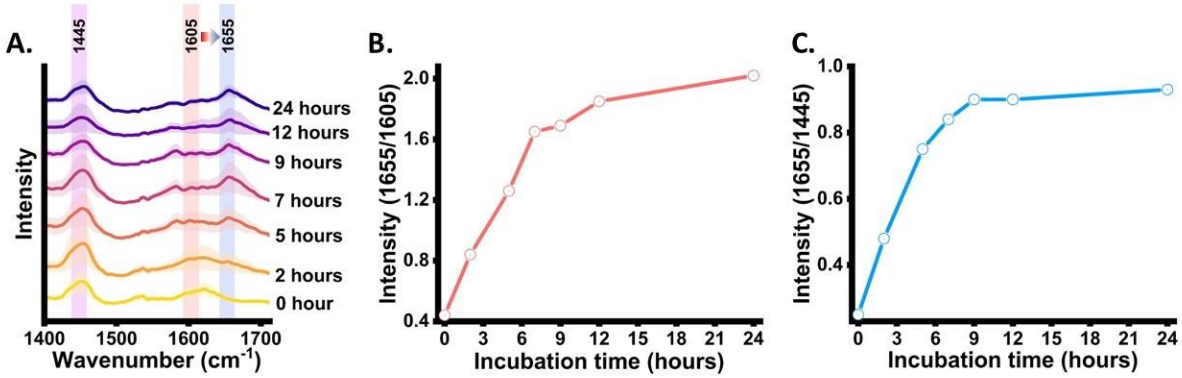

Fig 2. Lysis-free monitoring of de novo Single microbial cell oil synthesis using nascent UFA band as the tracer; (A) Mean Raman spectra showing blue-shift of Raman ^{13}C labelled UFA band (1605 cm^{-1}) towards unlabelled UFA band (1655 cm^{-1}) with incubation time, 1445 cm^{-1} acting as reference band for total lipid; (B) Ratiometric intensity (1655/1605) showing ^{12}C incorporation and turnover dynamics of nascent UFA in old UFA pool; (C) Ratiometric intensity (1655/1445) showing nascent UFA turnover in total intracellular lipid pool of the cell. (standard deviation is shown as shaded area).

band may change from strain to strain, in other species and growth parameters which needs to be optimized accordingly. As UFA are an essential component of SMCO composition and lipid body (also known as lipid droplet, oil body), therefore time-dependent intensity dynamics of the nascent UFA band at 1655 cm^{-1} can be the evident indicative tracer for de-novo SMCO synthesis and nascent SMCO turnover similar to the phenylalanine (1003 cm^{-1})[31–33,41,45] and Amide I (1667 cm^{-1}) [31–33,41,45] acting as Raman representative protein bands.

3.2. Validation of the nascent unsaturated fatty acid band from the cells

Further to validate that the detected nascent Raman band signal at 1655 cm^{-1} position is coming from unlabelled fatty acid we performed an inhibition assay (loss of function) using cerulenin, a well-known inhibitor of Fatty acid synthase (FAS), an important enzyme in the de-novo fatty acid synthesis pathway.[46] First we wanted to confirm that the used yeast strain is not resistant to cerulenin (50 µg/ml) treatment we performed the growth monitoring and the treatment was done at 7 hours post-inoculation, when cells are in the exponential phase of division, **Fig S1 (B)**. We observed a clear inhibitory effect of cerulenin on the growth of yeast. In the next step treatment was done at 0 hour and the average Raman spectra of cerulenin-treated cells at multiple incubation time points were acquired which shows a drastic reduction in signal at 1655 cm^{-1} attributed to nascent unsaturated band position as shown in **Fig. 3(A)**. The peak intensity at 1655 cm^{-1} is seen to be negligible from the cerulenin-treated cell of cerulenin and the intensity at 1605 cm^{-1} weakens with time. This supports the possible correlation between the peak at 1655 cm^{-1} and the nascent unsaturated fatty acid band in Raman spectra as cerulenin inhibits fatty acid synthesis. The mechanism of action of cerulenin inhibits the FAS enzyme leading to halted nascent fatty acid generation in cells which makes the cells to survive by depleting the stored cellular SMCO and ultimately leading to cell death.

The origin of 1655 cm^{-1} was also validated through “gain of function” assay. Here, we reversed the inhibitory effect of cerulenin on the cells by supplementing them with exogenous UFA.[46,47] This rescue of the treated cells by exogenous UFA supplementation occurs due to its preferential uptake for fulfilling the fatty acid scarcity due to inhibition of

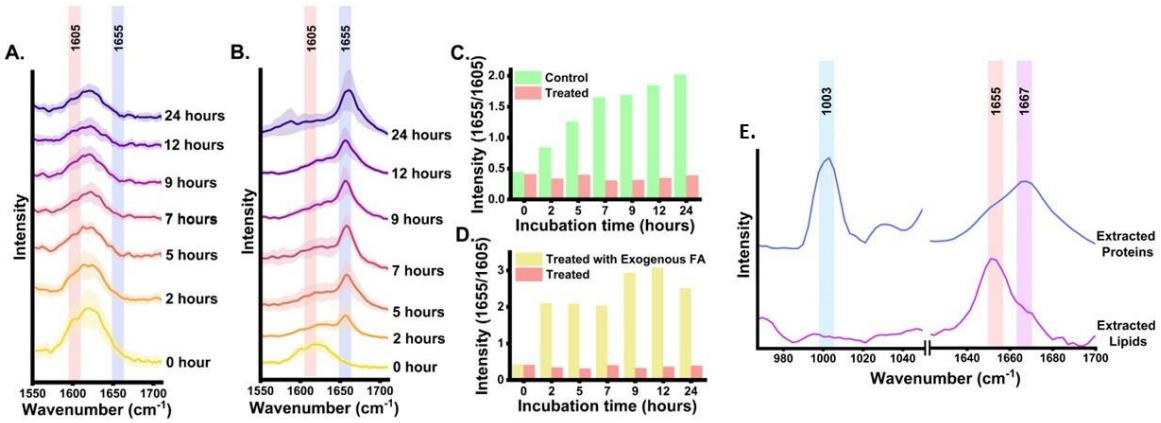

Fig 3. Validating the peak position at 1655 cm^{-1} is from nascent and unlabelled Unsaturated fatty acid; (A) Mean Raman spectra of Cerulenin treated Yeast cell; (B) Mean Raman spectra of Cerulenin treated Yeast cell supplemented with exogenous unsaturated fatty acid; (C) Bar plot showing relative ratiometric intensity (1655/1605) difference between control and cerulenin treated groups; (D) Bar plot showing relative ratiometric intensity (1655/1605) difference between cerulenin treated cells and cerulenin treated cells supplemented with exogenous unsaturated fatty acid. (E) Reference peak positions from extracted protein and lipid from cells after 24 hours; (standard deviation is shown as shaded area).

fatty acid sythesis.[46] We hypothesized that when treated cells incorporate external UFA for its rescue, we will observe a sudden spike in peak intensity at 1655 cm^{-1} from cells at early time points which is 2 hours in our study. Before supplementing it to cells we wanted to confirm that 1655 cm^{-1} is unique to UFA only, to address this concern we took the Raman spectra of some well-known standard saturated fatty acid and unsaturated fatty acids and did a ratio metric intensity quantification determining the degree of unsaturation shown in **Fig. S2**. The revived growth of cerulenin-treated cells by supplemented exogenous unsaturated fatty acid can be seen in **Fig S1(B)** which can be further enhanced when provided with saturated fatty acids**.** Raman spectra of rescued cells at 2 hours post-treatment, shows a highly intensified band at 1655 cm^{-1} which does not originate from *de novo* synthesis but from the uptake of exogenous UFA **Fig. 3(B)**. This provides further evidence in support of the fact that the Raman band position at 1655 cm^{-1} of cells indeed arises from unlabelled unsaturated fatty acid. Additionally, quantitative insight into the ratiometric unsaturated fatty acid band intensity (1655/1605) dynamics between the untreated cells and cerulenin-treated cells demonstrating the relative difference in nascent UFA content over time is shown **Fig. 3(C)**. Similarly, a relative quantitative ratio-metric analysis was performed for cerulenin-treated and rescued cells as shown in **Fig. 3(D)**. Furthermore, the band at 1655 cm^{-1} region is broad and this is well known that the spectral region is associated with adjacent protein band at around 1667 cm^{-1} (Amide I).[32,48] To address this aspect and validate that the band position 1655 cm^{-1} is predominately from UFA, we extracted the proteins and lipids from the reversely unlabelled cells after 24 hours and recorded Raman spectra. The spectral range cropped to the region of interest covering UFA and Amide I band is shown in **Fig. 3 (E)**. The highlighted peak position from the extracted unlabelled lipid is observed at around 1655 cm^{-1} and extracted unlabelled protein at around 1667 cm^{-1}. Further, 1003 cm^{-1} peak of phenylalanine was only observed in Raman spectra of extracted unlabelled protein which acts as a control.[32]

3.3. Visualisation and distribution of the *de novo* synthesized single microbial cell oil and its turnover over time.

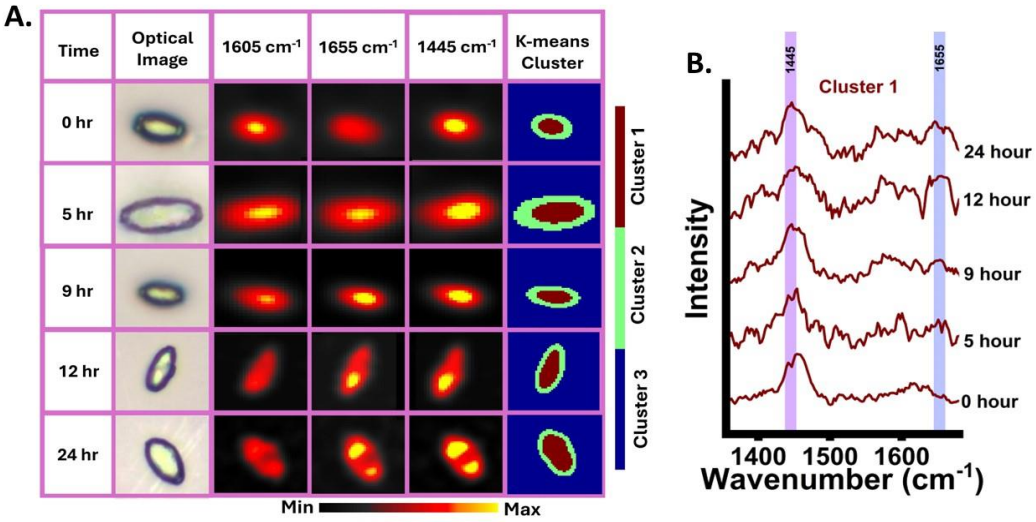

Fig 4. Visualization of single microbial cell oil turnover and distribution in yeast cells. (A) Raman image of de novo synthesized single microbial cell oil by metabolic incorporation of unlabelled glucose in Yeast cells and its turnover with time using 1605 cm^{-1}, 1655 cm^{-1} and 1445 cm^{-1}. K-means cluster image generated from hyperspectral image data with k=3. (B) Spectral component of Cluster 1 from different incubation time points.

After validating that the band at 1655 cm^{-1} is from nascent UFA and a potential tracer for SMCO synthesis, we further explored this band to map the distribution and dynamic of SMCO using RrSIP imaging, **Fig. 4 (A)**. Raman images of YL were generated from SMCO representative bands normalised intensity using false colour at different time intervals (0, 5, 9, 12 and 24 hours) as Raman intensity is proportional to biomolecular abundances. Corresponding optical image of the cells is also presented for a better understanding of cellular morphology. We observed Raman images of the total lipid signal at 1445 cm^{-1} and UFA signals (1605 and 1655 cm^{-1}) are giving coinciding signals in co-localized distribution and have high signal intensity at specific regions of cells are observed which can be interpreted as lipid body as per previous Raman images lipid body studies. [41,42,49,50] Low intensity SMCO band signal can be seen all over cellular regions indicating the presence of free fatty acid as its synthesis occurs in the cytoplasm which is later stored as TAG in lipid bodies and other forms of lipids as shown in **Fig. 4(A)**. At 0 hour the image shows high signal intensity distribution at 1605 cm^{-1}. At 5 hours we see equivalent intensity distribution from both 1605 and 1655 cm^{-1}. However, over time the distribution of 1655 cm^{-1} in the Raman image becomes significantly more and 1605 cm^{-1} reduces. This further demonstrates that by using the tracer band at 1655 cm^{-1}, the nascent SMCO distribution and turnover dynamics can be monitored over time. Further Clustered Raman image of the cells was generated by K-means cluster analysis (k=3). This unsupervised analysis of the hyperspectral image data set was done at each time interval without specifying any biomolecular bands. The hyperspectral image data set is decomposed into three different clusters with each cluster having statistically similar spectral information. Cluster 1 was seen to be originating from the intracellular region and the corresponding spectral component of cluster 1 is shown in **Fig. 4 (A) & (B).** The cluster 1 spectral components of each time point indicate the dynamic changes in the intensity of UFA at 1655 cm^{-1} from 0 hour to later incubation time points. As discussed earlier, at residual intensity remains at 1605 cm^{-1} as it is influenced by the presence of ergosterol at 1602 cm^{-1} and other biomolecular bands. The spectral component of Cluster 2 also shows biomolecular information and Cluster 3 shows signals from the background as shown in **Fig. S3 (A) & (B)**.

3.4. In situ monitoring of ex novo synthesis of single microbial cell oil synthesis from cooking oil and waste cooking oil source

Ex novo single-cell microbial oil synthesis is the capability of microbial cells to metabolize and incorporate the hydrophobic carbon sources such as oils, and alkanes and utilize it for cellular structure, metabolism, and energy storage.[51] Firstly, we grew the ^{13}C labelled YL in the carbon source-free synthetic medium with cooking oil namely palmolein oil and sunflower oil as the supplemented carbon source and incubated for 48 hours. Cooking oils are majorly composed of TAGs containing unsaturated fatty acid chains. Raman spectra of palmolein oil and sunflower oil used in our study as the hydrophobic carbon sources are shown in **Fig S4**., YL can secrete extracellular lipases which break down TAGs into glycerol and fatty acids. We recorded Raman spectra at 0, 12, 24 and 48 hours and monitored the lysis-free carbon flow from cooking oil to the SMCO pool validating *ex novo* SMCO synthesis and accumulation by tracking the dynamics of nascent 1655 cm^{-1} band. At 0 hours, we noticed residual band intensity at 1655 cm^{-1} indicating the cell's SMCO pool is ^{13}C labelled. Post inoculation at 12 hours we observed intensified band signal at 1655 cm^{-1} as shown in **Fig. 5 (A) and (B).** Over time at 24 and 48 hours post inoculation we see the intensified signal at SMCO bands at 1655 cm^{-1} and 1445 cm^{-1} and we see a rise in band intensity at 1740 cm^{-1} which has been assigned to the ester bond. This indicative increase in band intensity corroborates with the previous findings which have shown that the ex-novo synthesis induces higher assimilation of TAGs in YL.[51,52] This result aligns with the prior study, which

indicates feeding YL with oil as a carbon source has higher biomass yield when compared to YL grown in glucose with minimal medium.[53] To provide relative quantitative insight into the accumulation of the unsaturated fatty acid from the ex novo SMCO synthesis in the already existing UFA pool, the ratiometric integrated intensity at 1655/1605 was plotted with incubation time showing a linear increment with time with R square value of 0.99 and 0.98 as shown in **Fig. 5 (C) and (D)**.

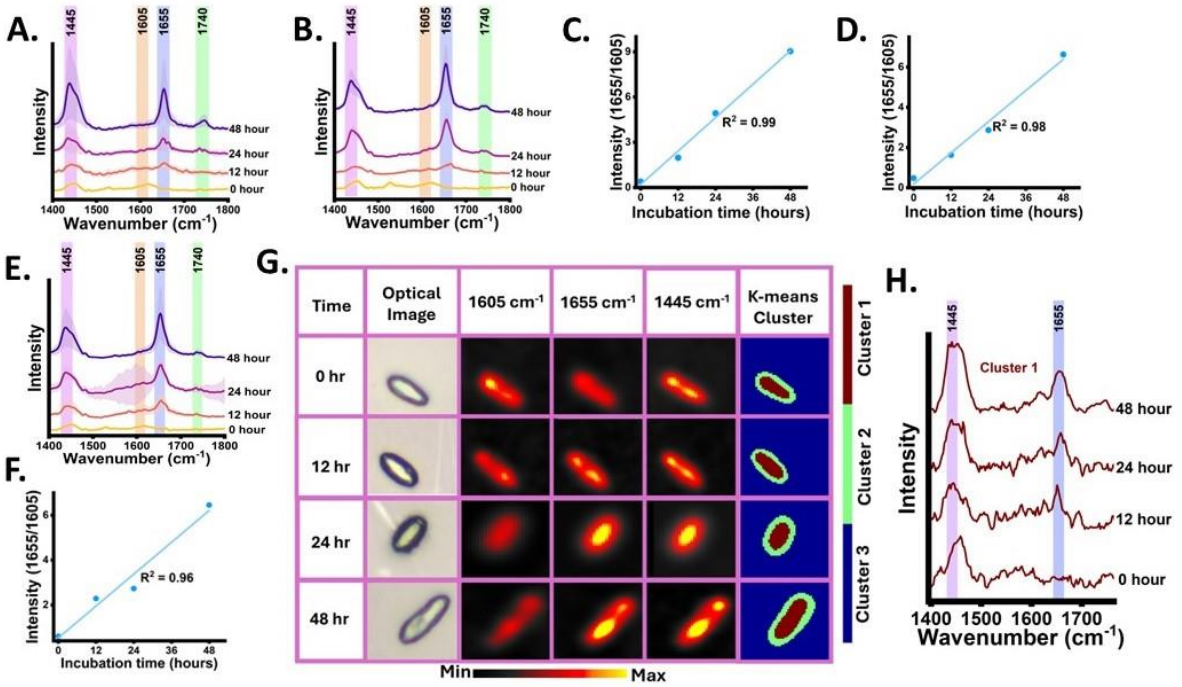

Fig 5. Lysis-free monitoring of ex novo synthesis of single cell microbial oil using nascent UFA band as the tracer; (A) & (B) Mean Raman spectra showing dynamics in SMCO bands with incubation time at different incubation time points grown in Palmolein and refined sunflower oil ; (C)&(D) Ratiometric intensity (1655/1605) showing metabolic ^{12}C carbon flow into nascent UFA from Palmolein and refined sunflower oil and turnover dynamics of nascent UFA in already existing UFA pool. (E) Mean Raman spectra showing dynamics in SMCO Raman bands different incubation time points grown in waste cooking oil; (F) Ratiometric intensity (1655/1605) showing metabolic ^{12}C carbon flow from waste cooking oil into nascent assimilated UFA pool of cells and turnover dynamics of nascent assimilated UFA in already existing UFA pool. (G) Raman image of de novo synthesized single microbial cell oil by metabolic incorporation of waste cooking oil in Yeast cells and its turnover and K-means cluster image generated from hyperspectral image data with k=3. (H) Spectral component of Cluster 1 from different incubation time points. (standard deviation is shown as shaded area).

After monitoring *the de novo and ex novo SMCO* synthesis in microbial cells targeting the tracer UFA band, our next goal was to analyse SMCO synthesis grown in synthetic media with WCO as the only carbon source. It is significant as SMCO produced from WCO helps in bioremediation as well as serves as sustainable biomass in biofuel and bioprocess industries. The WCO carbon source notably increases SMCO accumulation by folds when compared to cells grown in glucose which has been reported in a previous study.[11] Free fatty acids in WCO can be directly used for biodiesel production using conventional well-known methodologies such as enzymatic catalysis and noncatalytic transesterification routes. However, it is not a very feasible approach as WCO also contains, water, glycerides, aldehydes, organic acids and other organic compounds which hinders desirable Fatty acid methyl esters (FAME) yield and affects the quality of biodiesel. Therefore, microbial-based

bioremediation has been utilized for a cost-effective and improved FAME yield.[11] The Raman spectra of waste cooking oil is shown in **Fig. S5**. We have already validated the band intensity dynamics at 1655 cm^{-1} as a reliable efficient tracer to monitor the SMCO synthesis and accumulation. We took the Raman spectra from the cells grown in WCO at 0 hour, 12 hours, 24 hours and 48 hours as shown in **Fig 5 (E**). When compared to 0 hour, we observed increased peak intensity of 1655 cm^{-1} band at 12 hours and highly intensified peak at 24 and 48 hours. At 24 and 48 hours we also observed intensified peaks at 1445 and 1740 cm^{1}. This shows that the SMCO synthesis and assimilation from waste cooking oil. To provide relative quantitative validation into the assimilation of UFA and its turnover, the ratiometric integrated intensity at 1655/1605 was plotted with incubation time showing a linear increment with time with an R square value of 0.96 as shown in **Fig. 5(F)**. Further Raman image of the cells from the hyperspectral image data was generated at different time intervals from 0, 12, 24 and 48 hours as shown in **Fig 5 (G**). We monitored distribution of the intensity corresponding to SMCO which is 1605 cm^{-1}, 1655 cm^{-1} and 1445 cm^{-1} for investigating the distribution of UFA and nascent UFA assimilation dynamics. The Raman image gives us insight into SMCO distribution, localization of lipid bodies. The SMCO tracer band at 1655 cm^{-1} shows residual intensity distribution in Raman image at 0 hours which gets intensified with the incubation time, aids in visualizing the nascent SMCO assimilation and turnover from WCO. Further hyperspectral image data was subjected to k means (k=3) unsupervised algorithm forming 3 clusters of different colours. with each cluster having statistically similar information. The k means cluster image was generated with 3 clusters and the corresponding spectral components as shown in **Fig 5 (G).** The spectral pattern of components of different time intervals of cluster 1 as shown in **Fig. 5 (H)** which can be seen to be the group of pixels inside the cells corroborates with dynamics of 1655 cm^{-1} with time. The spectral component of Cluster 2 also shows biomolecular information and Cluster 3 shows signals from the background as shown in **FIG S5.** RrSIP-based in situ monitoring of SMCO synthesized from waste cooking oil gives qualitative as well as semi-quantitative insight in a lysis-free and non-destructive manner.

Previously, Raman spectroscopy has been used to study lipids in different microbes. In vivo lipid profiling of oil-producing microalgae *N. oleoabundans*, *B. braunii*, *B. sudeticus*, *C. reinhardtii*, and *T. minutus* was demonstrated by Seema et al using single-cell laser trapping Raman spectroscopy and quantitative assessment of the degree of unsaturation was done using intensity ratio (I_{1650} /I_{1440}).[43] Cheng et al have observed lipid droplets (lipid body) have a higher contrast at 1654 cm^{-1} position when compared to cytoplasm because of the lower contribution from the amide I band .[42] Hemanth et al have used Raman stable isotope probing-based imaging of single yeast cell *Schizosaccharomyces pombe* (*S. Pombe*) cells showing protein localization on lipid bodies targeting ^{13}C labelled nascent protein band at 967 cm^{-1} and lipid droplets at 1602 cm^{-1} and also reported band at 1654 cm^{-1} as unlabelled unsaturated lipid band.[41] Using Raman imaging of single cell *S. Pombe,* Shinshuke et al have shown the influence of high phospholipid contribution in 1655 cm^{-1} bands correlating it with the image from lipid band at 1440 cm^{-1}.[40] Yong et al studied the intracellular distribution and accumulation of lipids in nitrogen deficient condition of freshwater algae *Scenedesmus obliquus* using Raman Spectroscopy and imaging targeting band at 1445 cm^{-1}.[39] Tsuyoshi et al have shown the generated Raman images of the Lipid body of oleaginous diatom *Fistularia Solaris* Raman band at 1445 cm^{-1} was observed using Raman imaging and quantitative analysis of lipid unsaturation was studied using ratiometric intensity I_{1656} /$I_{1445.}$ Similarly waste cooking oil has been analysed using Raman spectroscopy without using microbial mediator studying vibrational mode at 1441, 1657 and 1747 cm^{-1}.[54] Even though the importance of lysis -free in situ monitoring of fatty acid biosynthesis is well known, there has not been many efforts. The overall study is a unique approach as it demonstrates a

novel application of reverse stable isotope probing combined with Raman spectroscopy and imaging for in-situ monitoring and visualization of single microbial cell oil synthesis which has never been done before. Further visualisation of nascent SMCO distribution and turnover was also analysed using Raman imaging. The RrSIP-based approach can be an intriguing adjunct for monitoring the waste cooking oil metabolic incorporation and nascent microbial oil dynamics in an extraction-free approach.

4. Conclusion:

Our findings suggest that the RrSIP coupled with Raman imaging holds immense potential as an adjunct lysis-free assay to analyse, monitor and visualize lipid dynamics in a qualitative and relatively quantitative manner. This approach is simple and cost-effective which can serve as a versatile tool in lipidomics for biofuel and bioprocess industrial applications.

Conflicts of Interest:

The author has no conflicts of interest to declare.

Acknowledgements:

This work was carried out under research grant project no (37/1739/23/EMR-II) supported by the Council of Scientific and Industrial Research (CSIR), Government of India and project no. IIRP-2023-1734 from the Indian Council of Medical Research (ICMR), Government of India. The authors are grateful for the seed funding to conduct the CESMI project at the University of Eastern Finland, provided by the Finnish Ministry of Education and Culture through the Finnish Indian Consortia for Research and Education (FICORE) Global pilot network. We also thank the Finnish National Agency for Education's Team Knowledge Finland (TFK) programme for their financial support to the project 'DEDUCE' (grant number 78/116/2022).

References:

1 A. Mannu, M. Ferro, M. E. Di Pietro and A. Mele, *Sci Prog*, 2019, **102**, 153–160.

2 O. Awogbemi, D. V. Von Kallon, V. S. Aigbodion and S. Panda, *Case Studies in Chemical and Environmental Engineering*, 2021, **4**, 100158.

3 X. Cui, N. Sun, P. Cao, J. Guo and P. Ming, *J Manuf Process*, 2022, **77**, 508–524.

4 G. De Feo, C. Ferrara, L. Giordano and L. S. Ossèo, *Recycling*, 2023, **8**, 64.

5 A. H. Hashem, A. M. Khattab and M. Abdelraof, *Biomass Convers Biorefin*, 2023, **13**, 16711–16721.

6 Q.-Q. Zhang, B.-X. Cai, W.-J. Xu, H.-Z. Gang, J.-F. Liu, S.-Z. Yang and B.-Z. Mu, *Sci Rep*, 2015, **5**, 9971.

7 A. Mannu, S. Garroni, J. Ibanez Porras and A. Mele, *Processes*, 2020, **8**, 366.

8 Y. Li, Z. Cheng, C. Zhao, C. Gao, W. Song, L. Liu and X. Chen, *ACS Synth Biol*, 2021, **10**, 1966–1979.

9 R. Marchetti, C. Vasmara, L. Bertin and F. Fiume, *Appl Microbiol Biotechnol*, 2020, **104**, 2833–2856.

10 J. Karlo, R. Prasad and S. P. Singh, *J Agric Food Res*, 2023, **11**, 100482.

11 G. Raut, S. Jagtap, V. R. Kumar and A. RaviKumar, *Biomass Convers Biorefin*, , DOI:10.1007/s13399-022-02610-1.

12 B. Zieniuk and A. Fabiszewska, *World J Microbiol Biotechnol*, 2018, **35**, 10.

13 A. Rywińska, P. Juszczyk, M. Wojtatowicz, M. Robak, Z. Lazar, L. Tomaszewska and W. Rymowicz, *Biomass Bioenergy*, 2013, **48**, 148–166.

14 Y.-L. Jia, L.-R. Wang, Z.-X. Zhang, Y. Gu and X.-M. Sun, *Crit Rev Food Sci Nutr*, 2022, **62**, 8920–8934.

15 C. Ratledge and J. P. Wynn, 2002, pp. 1–52.

16 G. Katre, C. Joshi, M. Khot, S. Zinjarde and A. RaviKumar, *AMB Express*, 2012, **2**, 36.

17 P. Gajdoš, R. Ledesma-Amaro, J.-M. Nicaud, M. Čertík and T. Rossignol, *FEMS Yeast Res*, 2016, **16**, fow062.

18 A. Beopoulos, Z. Mrozova, F. Thevenieau, M.-T. Le Dall, I. Hapala, S. Papanikolaou, T. Chardot and J.-M. Nicaud, *Appl Environ Microbiol*, 2008, **74**, 7779–7789.

19 Y. Pang, Y. Zhao, S. Li, Y. Zhao, J. Li, Z. Hu, C. Zhang, D. Xiao and A. Yu, *Biotechnol Biofuels*, 2019, **12**, 241.

20 L. Mitrea, L.-F. Călinoiu, B.-E. Teleky, K. Szabo, A.-G. Martău, B.-E. Ştefănescu, F.-V. Dulf and D.-C. Vodnar, *Environ Technol Innov*, 2022, **28**, 102943.

21 M. Groenewald, T. Boekhout, C. Neuvéglise, C. Gaillardin, P. W. M. van Dijck and M. Wyss, *Crit Rev Microbiol*, 2014, **40**, 187–206.

22 F. Thevenieau and J.-M. Nicaud, *OCL*, 2013, **20**, D603.

23 T. M. N. Ta, C. Romero-Guido, T. H. Phan, H. D. Tran, H. T. Dinh and Y. Waché, *AIMS Biophys*, 2022, **9**, 257–270.

24 N. Morin, Q. Czerwiec, J. Nicaud, C. Neuvéglise and T. Rossignol, *Yeast*, 2020, **37**, 348–355.

25 A. Daskalaki, N. Perdikouli, D. Aggeli and G. Aggelis, *Appl Microbiol Biotechnol*, 2019, **103**, 8585–8596.

26 P. Radha, S. Narayanan, A. Chaudhuri, S. Anjum, D. L. Thomas, R. Pandey and K. Ramani, *Biomass Convers Biorefin*, 2023, **13**, 1–12.

27 X. Niehus, A.-M. Crutz-Le Coq, G. Sandoval, J.-M. Nicaud and R. Ledesma-Amaro, *Biotechnol Biofuels*, 2018, **11**, 11.

28 Y. Wang, W. E. Huang, L. Cui and M. Wagner, *Curr Opin Biotechnol*, 2016, **41**, 34–42.

29 S. A. Eichorst, F. Strasser, T. Woyke, A. Schintlmeister, M. Wagner and D. Woebken, *FEMS Microbiol Ecol*, 2015, **91**, fiv106.

30 Karlo Jiro, Gupta Aryan and Singh Surya Pratap., *Analyst*, , DOI:https://doi.org/10.1039/D4AN00203B.

31 Y. Wang, Y. Song, Y. Tao, H. Muhamadali, R. Goodacre, N.-Y. Zhou, G. M. Preston, J. Xu and W. E. Huang, *Anal Chem*, 2016, **88**, 9443–9450.

32 J. Karlo, A. K. Dhillon, S. Siddhanta and S. P. Singh, *J Biophotonics*, , DOI:10.1002/jbio.202300341.

33 M. Chisanga, H. Muhamadali, D. McDougall, Y. Xu, N. Lockyer and R. Goodacre, *Analyst*, 2021, **146**, 1734–1746.

34 V. Tsakraklides, A. Kamineni, A. L. Consiglio, K. MacEwen, J. Friedlander, H. G. Blitzblau, M. A. Hamilton, D. V. Crabtree, A. Su, J. Afshar, J. E. Sullivan, W. G. LaTouf, C. R. South, E. H. Greenhagen, A. J. Shaw and E. E. Brevnova, *Biotechnol Biofuels*, 2018, **11**, 131.

35 E. Carsanba, S. Papanikolaou, P. Fickers and H. Erten, *Microorganisms*, , DOI:10.3390/microorganisms8071054.

36 R. M. Olayide Israel, Extraction of Lipids from Yeast.

37 T. von der Haar, *PLoS One*, 2007, **2**, e1078.

38 N. Mobaraki and J. M. Amigo, *Chemometrics and Intelligent Laboratory Systems*, 2018, **172**, 174–187.

39 Y. Shao, H. Fang, H. Zhou, Q. Wang, Y. Zhu and Y. He, *Biotechnol Biofuels*, 2017, **10**, 300.

40 C.-K. Huang, H. Hamaguchi and S. Shigeto, *Chemical Communications*, 2011, **47**, 9423.

41 H. N. Noothalapati Venkata and S. Shigeto, *Chem Biol*, 2012, **19**, 1373–1380.

42 M. N. Slipchenko, T. T. Le, H. Chen and J.-X. Cheng, *J Phys Chem B*, 2009, **113**, 7681–7686.

43 H. Wu, J. Volponi, A. Oliver, A. Parikh, B. Simmons and S. Singh, *Nature Precedings*, , DOI:10.1038/npre.2010.4428.1.

44 L. Chiu, F. Hullin-Matsuda, T. Kobayashi, H. Torii and H. Hamaguchi, *J Biophotonics*, 2012, **5**, 724–728.

45 M. Chisanga, H. Muhamadali, D. McDougall, Y. Xu, N. Lockyer and R. Goodacre, *Analyst*, 2021, **146**, 1734–1746.

46 L. N. Nguyen and J. D. Nosanchuk, *Commun Integr Biol*, 2011, **4**, 631–2.

47 J. Awaya, T. Ohno, H. Ohno and S. Ōmura, *Biochimica et Biophysica Acta (BBA) - Lipids and Lipid Metabolism*, 1975, **409**, 267–273.

48 J. Karlo, A. K. Dhillon, S. Siddhanta and S. P. Singh, *J Biophotonics*, , DOI:10.1002/jbio.202200341.

49 M. Uematsu and T. Shimizu, *Commun Biol*, 2021, **4**, 1176.

50 K. Kochan, H. Peng, B. R. Wood and V. S. Haritos, *Biotechnol Biofuels*, 2018, **11**, 106.

51 Fabiszewska, Misiukiewicz-Stępień, Paplińska-Goryca, Zieniuk and Białecka-Florjańczyk, *Biomolecules*, 2019, **9**, 685.

52 A. Beopoulos, T. Chardot and J.-M. Nicaud, *Biochimie*, 2009, **91**, 692–696.

53 A. M. Worland, J. J. Czajka, Y. Xing, W. F. Harper, A. Moore, Z. Xiao, Z. Han, Y. Wang, W. W. Su and Y. J. Tang, *Metab Eng Commun*, 2020, **11**, e00130.

54 H. Jin, H. Li, Z. Yin, Y. Zhu, A. Lu, D. Zhao and C. Li, *Food Chem*, 2021, **362**, 130191.

Supplementary Figures:

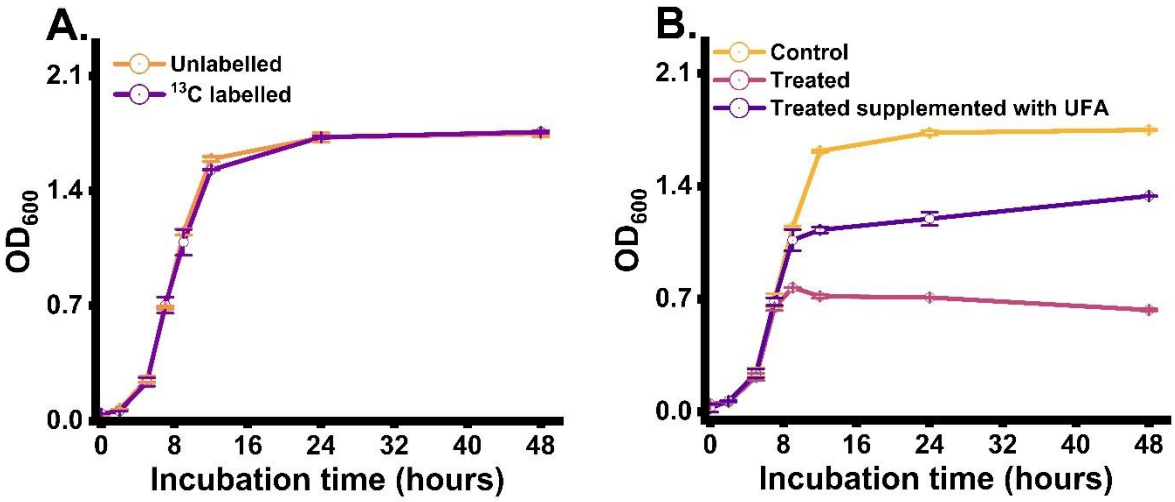

Fig S1. Growth monitoring of *Yarrowia Lipolytica* (A) YL grown in carbon source-free synthetic medium with unlabelled glucose and ^{13}C labelled glucose as the sole carbon source supplement. (B) YL grown in culture medium without cerulenin treatment, with cerulenin treatment at 8 hours and cerulenin treated medium with exogenous unsaturated fatty acid.

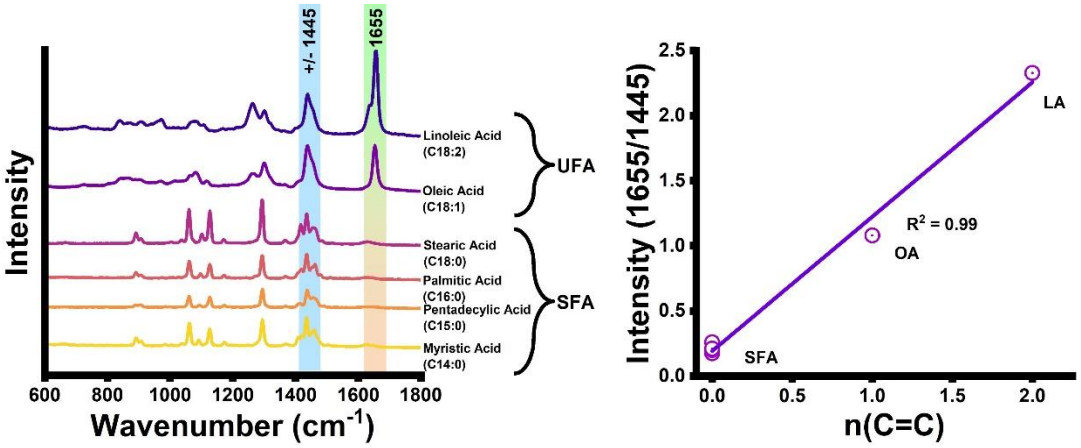

Fig S2. Raman analysis of standard saturated and unsaturated fatty acid. A. Raman spectra of fatty acid B. Quantifying degree of unsaturation from Raman spectra by plotting the ratiometric Raman intensity (1655/1445) to the number of C=C. SFA = Saturated fatty Acid; UFA = Unsaturated Fatty Acid; OA = Oleic Acid; LA = Linoleic Acid.

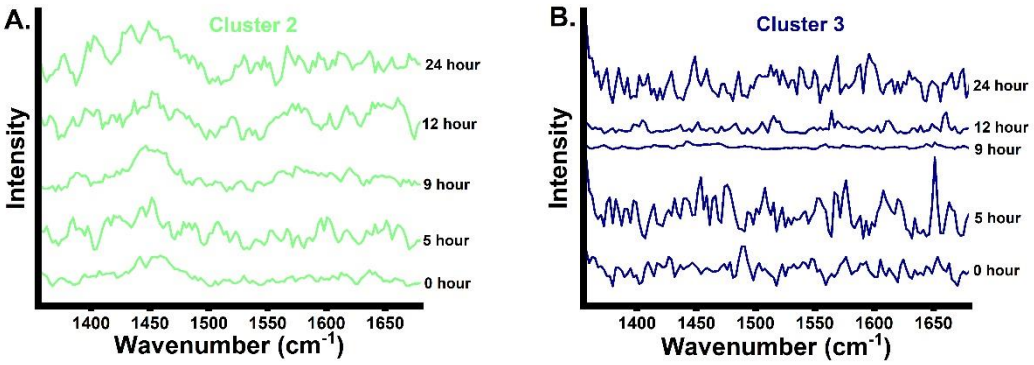

Fig S3. K- means cluster components of different time points; (A) Cluster 2 (B) Cluster 3

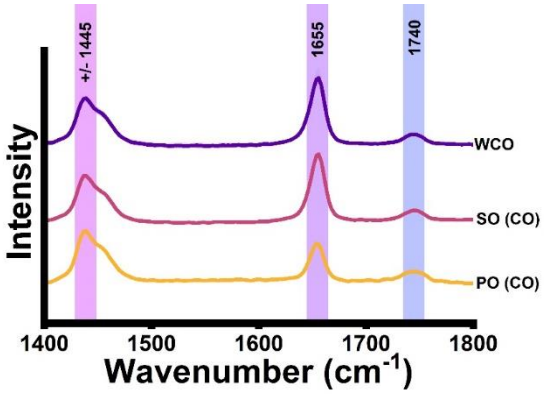

Fig S4. Raman spectra of Oils used as only carbon source; Cooking Oil (CO) - Palmolein Oil (PO) and Sunflower Oil (SO) and Waste cooking oil (WCO).

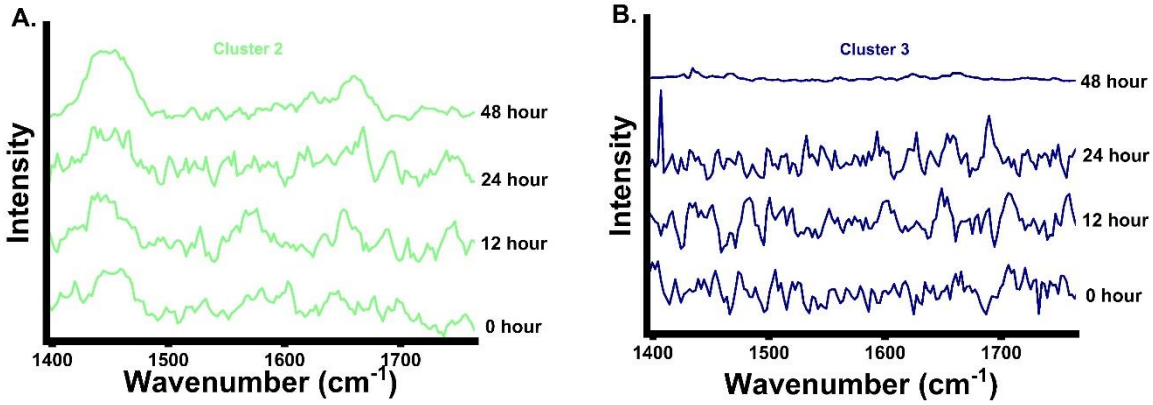

Fig S5. K- means cluster components of different time points; (A) Cluster 2 (B) Cluster 3